



Deep structural heterogeneities and the tectonic evolution of the Abruzzi region (Central Apennines, Italy) revealed by microseismicity, seismic tomography, and teleseismic receiver functions

C. Chiarabba^a, S. Bagh^a, I. Bianchi^{a,*}, P. De Gori^a, M. Barchi^b

^a Istituto Nazionale di Geofisica e Vulcanologia, Rome, Italy

^b Università degli Studi di Perugia, Italy

ARTICLE INFO

Article history:

Received 16 June 2009

Received in revised form 2 March 2010

Accepted 16 April 2010

Available online 21 May 2010

Editor: R.D. van der Hilst

Keywords:

microseismicity
tomography
receiver functions
Abruzzi

ABSTRACT

The crustal structure of central Apennines (Italy) is still poorly defined, leaving uncertainties on the tectonic style (thin or thick-skinned) responsible for the development of the thrust-and-fold belt. The today active extension, which replaced compression since early Quaternary, is presumably influenced by the pre-existing structure that yields location and segmentation of the fault system. To focus on such issues, we computed P- and S-wave velocity models of the crust by using the independent methodologies of local earthquakes tomography and teleseismic receiver function. We document strong lateral and vertical heterogeneities that define shallow, imbricate sheets of the Mesozoic cover that overlay exceptionally high V_p and high V_s bodies. These bodies can be interpreted as either dolomitic or, partially hydrated, mafic rocks. The two alternative interpretations respectively imply an ultra-thick deposition of dolomitic rocks in the hanging wall of Triassic normal fault or a deep exhumation of the Pre-Mesozoic basement during the early Mesozoic sin-rift tectonic. In both cases, these bodies influenced the evolution of the thrust-and-fold belt. Very remarkably, active normal faults, like those ruptured during the still ongoing 2009 L'Aquila sequence, concentrate at the border of these bodies, suggesting that they have an active role in the segmentation of the normal fault system. The rheological behavior of such high V_p high V_s bodies, weak or strong, is still uncertain, but of utmost importance to understand the risk of future normal faulting earthquakes.

© 2010 Elsevier B.V. All rights reserved.

1. Introduction

This study has been performed before the April 06, 2009 Mw6.3 L'Aquila earthquake. Here we present tomographic results from a seismic passive experiment executed in the Abruzzi region during 2003 and 2004, whose main goal was the definition of crustal structure and seismicity. In addition, we show the location of a sub-set of aftershocks of the 2009 seismic sequence, obtained with this 3D model, and use them to infer insight on the seismotectonics of the region.

The central Apennines Mio-Pliocene thrust-and-fold belt was formed during the westward subduction of the Adria slab, after the consumption of the Tethys Ocean. The resistance of the continental lithosphere in subducting is believed to be the cause of slab break-off or slab windows (see Lucente et al., 1999; Di Stefano et al., 2009) and affects the evolution and tectonic style of the belt. After the belt build-up, extension takes place in regions formerly subjected to compression (Ghiesetti and Vezzani, 1997; Galadini and Galli, 2000; D'Agostino

et al., 2001; Galadini and Galli, 1999). An almost continuous but segmented NW-trending normal fault runs along the Apennines right above the contacts at Moho depth (see Di Stefano et al., 2009) between the Adria and Tyrrhenian plates (see Fig. 1). In the Abruzzi region, large and destructive normal faulting earthquakes, such as the Mw 6.7, 1915 Avezzano earthquake (Ward and Valensise, 1989; Amoroso et al., 1998) and the April 06 2009 Mw6.3 L'Aquila earthquake, occur on several parallel and adjacent NW-trending fault segments (e.g. Barchi et al., 2000; Galadini and Galli, 2000; D'Addezio et al., 2002; Roberts and Michetti, 2004; Chiarabba et al., 2009; Atzori et al., 2009). Despite this vocation to large destructive earthquakes, the background seismicity in central Apennines is scarce as evidenced by permanent seismic networks (Chiarabba et al., 2005; De Luca et al., 2009) and temporary experiments (Bagh et al., 2007).

The main goal of this study is to shed light on the structure of the crust, contributing to understand: i) whether thin- or thick-skinned tectonic models (see Coward, 1983; Calamita and Deiana, 1988; Butler et al., 2004; and Scrocca et al., 2005, for a review) best apply to explain the belt evolution, ii) how long the pre-existing structure influences fault segmentation and seismicity occurrence. Today most of the information on the central Apennines belt structure came from surface geology data and seismic profiles, which have a prevalent

* Corresponding author.

E-mail address: irene.bianchi@ingv.it (I. Bianchi).

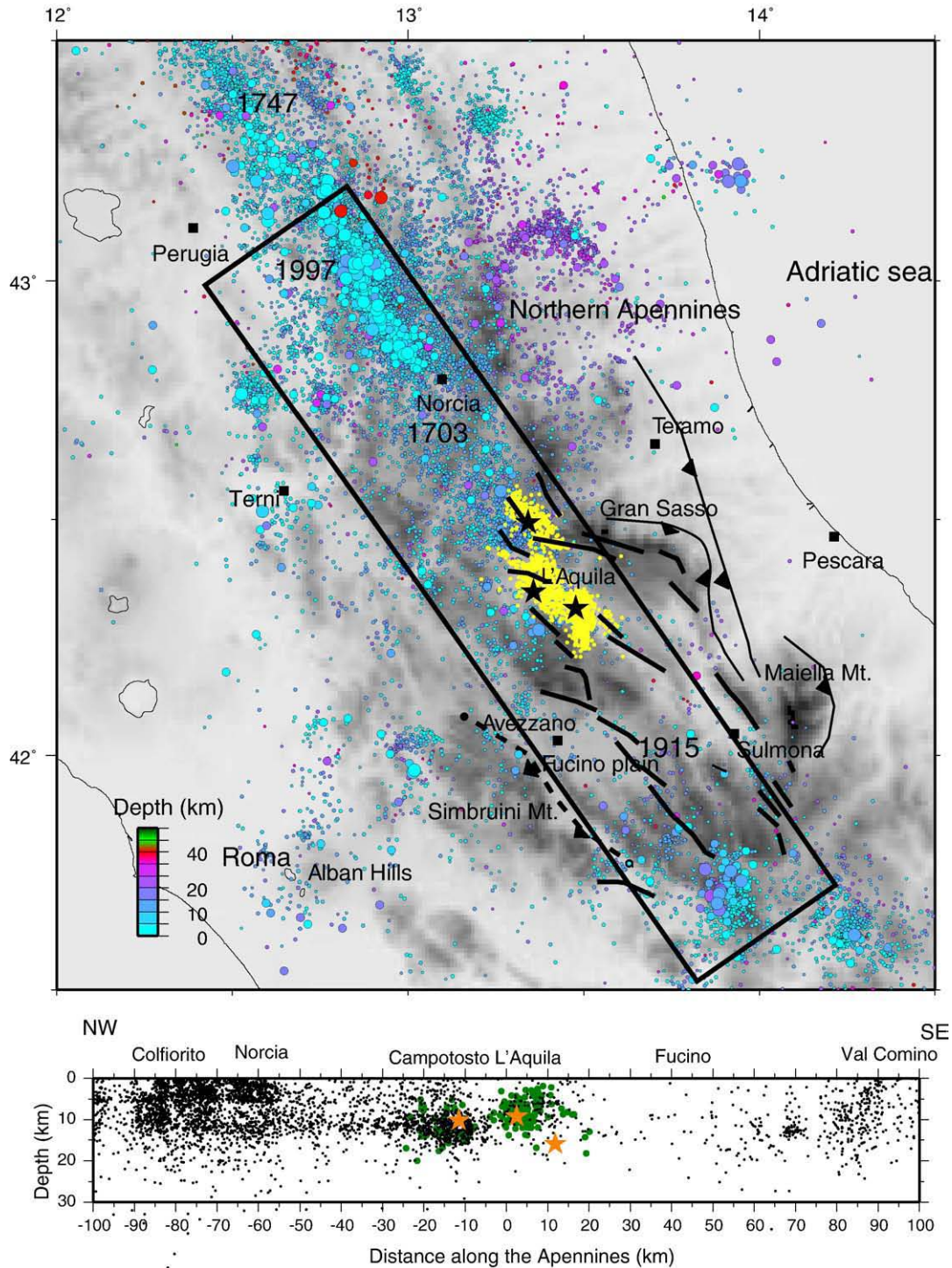


Fig. 1. Map of the instrumental seismicity of central northern Apennines (period 1980–2000, from the CSI 1.1 catalogue, see www.ingv.it/CSI1.1, updated to 2008). Colour codes for different hypocentral depths and circle dimension for magnitude smaller or larger than 3.9. The date of the most recent $M > 6.0$ earthquakes on each segment of the Apenninic fault system is reported. The main tectonic lines of the study region are shown along with the mainshocks (black stars) and aftershocks of the 2009 seismic sequence (in yellow). Note that the seismicity in the Abruzzi region has been low in the past 28 years. The lower panel shows a vertical section of the seismicity across the belt. The green dots are the aftershocks and the orange stars are the mainshocks of the L'Aquila 2009 earthquake.

resolution for shallow features (CROP-03, CROP-11 and CROP-04, Pialli et al., 1998; Barchi et al., 1998a,b; Mazzotti et al., 1999; Calamita et al., 2004; Scrocca et al., 2005; Billi et al., 2006; Patacca et al., 2008, see Fig. 1). In this paper, we compute the crustal structure by using local earthquake tomography and receiver function modelling, which give independent, complementary and consistent information. The inversion of body wave arrival times, from local earthquakes recorded at permanent and temporary seismic networks, yields original and

well resolved V_p and V_p/V_s images down to 15–18 km depth, thus directly illuminating the basement of the Mesozoic cover. To corroborate the reliability of tomographic pictures and extend the reconstruction of the structure to the entire crust, we analyze receiver functions (RF) of teleseismic waveforms recorded at broadband permanent stations of the INGV seismic network. These techniques are widely used worldwide to define the 1D and 3D V_s structure underneath seismic stations (Sherrington et al., 2004; Savage et al.,

2007). The recently increased number of permanent broadband stations in central Apennines makes such effort very feasible and straightforward. The combination of the two methodologies gives reciprocal constraints and support for the reliability of the retrieved deep structure (see *Piana Agostinetti and Chiarabba, 2008*).

2. Geological and seismotectonic setting

The Apennines belt is a paired tectonic belt, with extension in the orogenic hinterland balancing (more or less) the orogenic contraction on the foreland side (*Frepoli and Amato, 1997; Decandia et al., 1998; Montone et al., 2004*). Due to the eastward migration of the compressive front started in early Miocene, the extension develops on areas previously deformed by the compressive tectonics (*Elter et al., 1975; Barchi et al., 1998a,b; Cavinato and De Celles, 1999; Galadini*

and Galli, 2000). Although at a broad scale the evolution of the Apennines is believed to follow the eastward migration of the Adria slab, the absence of high V_p anomalies in the uppermost mantle suggests that a slab window developed after the continental collision (*Lucente et al., 1999; Di Stefano et al., 2009*).

Active extension follows the main topographic ridge and is concentrated in a belt which width varies along the strike of the peninsula (*Selvaggi et al., 1997*) and reaches its greatest width (>50 km) in the central Apennines (*Fig. 1*). In the literature, there is (or there was before the 2009 L'Aquila earthquake) a prevailing consensus that the late Pleistocene–Holocene deformation is accommodated by two major sub-parallel normal fault systems (the eastern and western normal fault systems, WNFS and ENFS see *Vezzani and Ghisetti, 1998; Barchi et al., 2000; Galadini and Galli, 2000; Boncio et al., 2004; Roberts and Michetti, 2004*). These SW-dipping normal

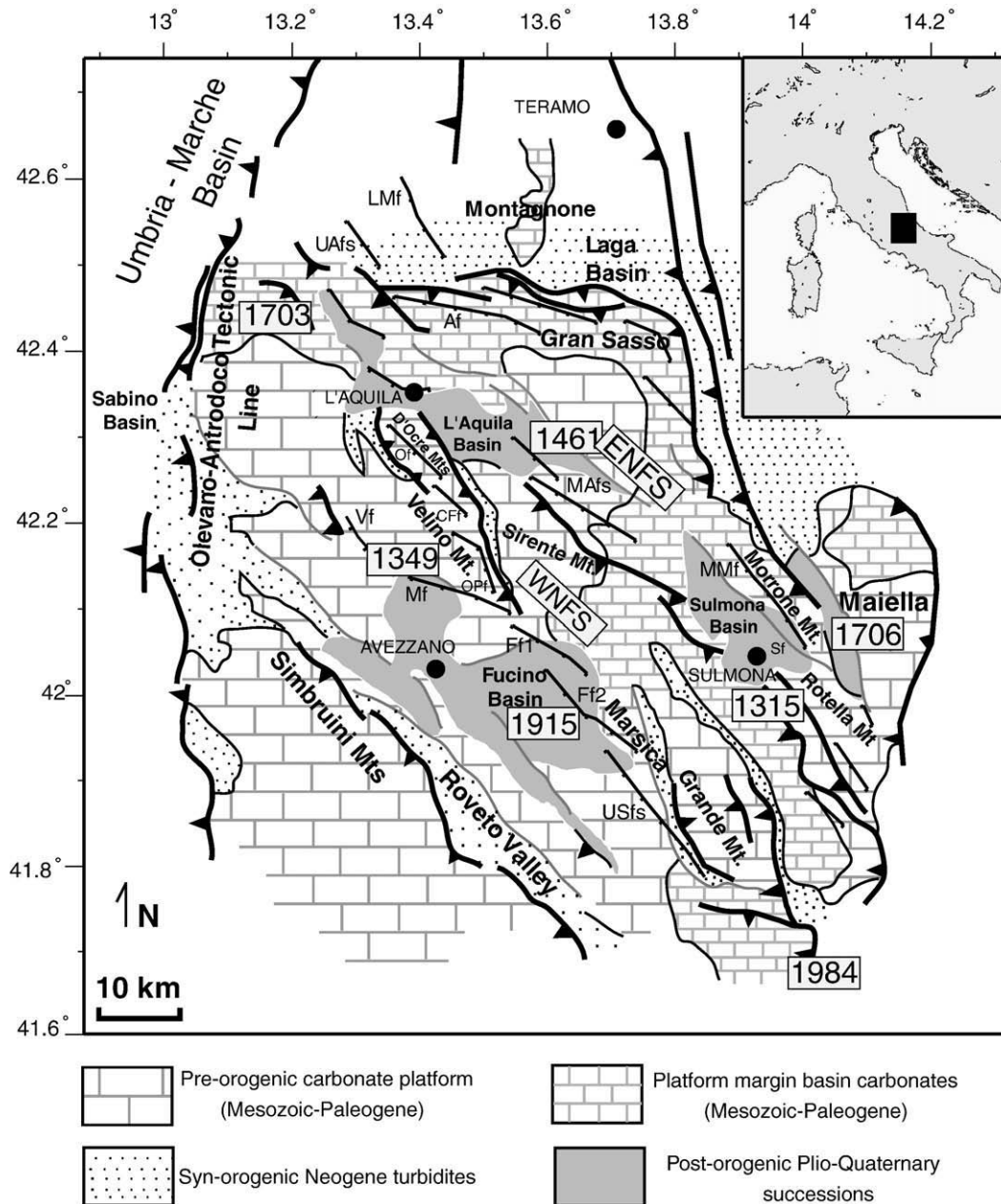


Fig. 2. Structural sketch of central Apennines. Gray and thick black lines represent extensional structures and thrusts, respectively. Thin black lines represent active normal faults (*Barchi et al., 2000*): LMf, Laga Mts. fault; UAfs, Upper Aterno fault system; Ff (1,2), Fucino fault system; USfs, Upper Sangro fault system; MMf, Mt. Morrone fault; Af, Assergi fault; MAfs, Middle Aterno valley fault system; OPf, Ovidoli Pezza fault; Mf, Magnola fault; CFF, Campo Felice fault; Of, Ocre fault; Vf, Velino fault. Locations of large historical earthquakes are also shown (CPTI working group, 1999).

faults presumably controlled the formation of intermountain basins (l'Aquila, Sulmona and Fucino basins, see Fig. 2), that are unconformably covered by late Pliocene–Quaternary continental deposits (Cavinato and De Celles, 1999; Galadini and Galli, 2000). The ENFS bounds the Laga and Gran Sasso massifs and the Sulmona basin, whereas the WNFS is elongated from the northern end of the l'Aquila basin to the Fucino basin and the Marsica region (D'Agostino et al., 2001). Preliminary information on the 2009 l'Aquila earthquake seems more consistent with the existence of a normal fault system located in between those formerly suggested (Chiarabba et al., 2009). This new information raises concerns on the role played by the extensively mapped Quaternary faults.

In the past thousand years, destructive earthquakes originated in the region (see Fig. 2, the 1349, I=XI–X; the 1461, l'Aquila, I=X and the 1703, I=X, working group CPTI, 1999). The most recent significant earthquakes are the Fucino 1915 Mw=6.7 earthquake (Ward and Valensise, 1989; Michetti et al., 1996; Galadini and Galli, 1999) and the 1984 moderate magnitude ($M_L=5.8$) normal faulting event of the Sangro Valley (Pace et al., 2002). Holocene activity has been recognized by paleoseismology on the Fucino and the contiguous faults of the WNFS (Pantosti et al., 1996; Galadini and Galli, 2000). The ENFS shows evidence of Late Pleistocene to Holocene activity (Galadini and Galli, 2000) but historical earthquakes are not clearly associated to these faults.

The central Apennines comprises the southern Tethys passive margin units: basins, ramps and structural highs of Permo-Triassic to Miocene age (Dondi et al., 1966; Parotto and Pratorlon, 1975), dominated by platform, margin and basin carbonate rocks. During the Liassic extension, the central Italy split along the Olevano–Antròdoco–Sibillini (O–A–S) salient into two paleo-tectonic domains (Fig. 2): the Lazio–Abruzzo carbonate platform (the study region) and Umbria–Marche–Sabina pelagic basin (Castellarin et al., 1982; Calamita and Deiana, 1988; Decandia et al., 2002; Bigi and Pisani, 2005). The sedimentary cover consists of (from bottom to top): 1) Late Triassic alternated anhydrites and dolomites (e.g. Burano formation; Martinis and Pieri, 1964; Parotto and Pratorlon, 1975); 2) a 3–4 km thick Jurassic to Paleogene laterally heterogeneous successions mainly deposited on adjacent paleogeographic realms, comprising shallow water platform carbonates as well as local deep basinal successions (Parotto and Pratorlon, 1975; Patacca et al., 2008).

The Mio-Pliocene compression was accommodated by first order (the O–A–S, the Gran Sasso, the Simbruini, the Teramo and Maiella thrusts, Fig. 2) and second order features (the Mts. D'Ocre and Sirente, the Rotella and Grande Mts. thrusts, Fig. 2). The strong variability in the thrust belt architecture suggests that the paleogeography of the passive continental margin controlled the evolution of the belt (Calamita et al., 2003).

3. Local earthquake tomography

The inversion of P and S–P arrival times has been computed by using the technique developed originally by Thurber (1983) and Um and Thurber (1987), as modified by Eberhart-Phillips (1993) and Eberhart-Phillips and Reyners (1997). The technique uses P-wave and S–P arrival times to invert simultaneously for hypocentral and velocity (Vp and Vp/Vs) parameters. The velocity is continuously defined within the volume by using a linear interpolation among the adjacent nodes (Fig. 3). The solution is obtained by using an iterative damped least squares algorithm. The damping value is chosen to optimize the data misfit and model complexity. The procedure is iterated until the variance improvement is retained to be significant, according to an *f*-test.

In this study, local earthquake data ($M_L < 3.7$) recorded by temporary local seismic networks operative between April 2003 and September 2004 (Bagh et al., 2007) and in the Alban Hills volcano are used along with permanent seismic stations belonging to both the

INGV national network and the Abruzzi regional network (De Luca et al., 2009), for a total of 139 stations, to compute three-dimensional Vp and Vp/Vs models (Fig. 3). A total of 786 local earthquakes is selected based on the following criteria: a root-mean-square (RMS) residual less than 0.5 s, hypocentral errors less than 2.0 km, azimuthal gap less than 180°, and at least 12 P-wave readings. The solution of model parameters is performed by iterative damped least squares inversion, where the damping parameters are selected empirically by optimizing data variance reduction and model complexity. In our inversion, we used a total of 12,317 P-wave and 8,882 S–P arrival times to solve for 2048 velocity and 3144 hypocentral parameters using damping values equal to 40 for Vp, 60 for Vp/Vs and 90 for station corrections. As a starting 1-D velocity model, we used the model computed for the central Apennines by Bagh et al. (2007). The velocity model is parameterized by assigning the 1-D model values to the nodes of a 3-D grid. The horizontal grid area is around 160 km both in X and Y directions with a node spacing of 10 km in the central part of the grid and 20 km in the less resolved model periphery (Fig. 3). In the vertical direction, the model is divided into six layers located at 0, 4, 8, 12, 16 and 20 km depth. We progressively under-weighted arrival times for seismic rays traveling more than 80 km and not use them for distance greater than 110 km. After four iterations, we obtain a final rms value of 0.19 s with a variance improvement equal to 46%. The quality of velocity models has been verified with the complete analysis of the resolution matrix (Menke, 1989) and synthetic test that focus on the reliability of the recovered deep ultra-fast bodies (see Appendix A). We inspect each row of the resolution matrix to verify the smearing of the matrix around the diagonal elements (spread function) and sharpness of the averaging vector (Toomey and Foulger, 1989). A delta-like averaging vector characterizes a perfectly resolved node, with more than 70% of the smearing contour around the diagonal element. Then, we select the value of spread function that encompasses the well-resolved parameters (see Fig. A1). In our inversion, all the parameters with values smaller than 2 are well resolved, condition that is verified in most of the model.

3.1. Velocity models

Fig. 4 (a and b) shows the Vp and Vp/Vs models together with the relocated events. The velocity anomalies described in this section are located inside the well-resolved crustal volume.

At 0 km depth (Fig. 4a), the low velocity regions (Vp lower than 4.8 km/s) correspond with the main Plio-Quaternary sedimentary basins of the Abruzzi Apennines (l'Aquila, Sulmona and Fucino basins see the red anomalies in the 0-km-depth layer of Fig. 4) and that surrounding the Alban Hills volcano. Other secondary features are NNE-trending low velocity anomalies at the boundary of the platform margin carbonate rocks to the W of the Sulmona and Fucino basins. A positive velocity anomaly is also present in the northeastern part of the model; in correspondence with the Montagnone Mt. and Teramo thrusts (anomaly A in Fig. 4). Regions of relatively high velocity values (Vp larger than 5.0 km/s) are mostly correspondent with the Mesozoic platform carbonates, widely exposed in the Abruzzi Apennines (see Parotto and Pratorlon, 1975). High Vp regions are found beneath the Montagna Grande, the M. Morrone and Monti D'Ocre and Sirente massifs (anomaly B in Fig. 4). Since narrow and small, Neogene flysch basins are not distinguishable as low velocity anomalies, except for the flysch outcrops located to the north-west of the Simbruini Mts (anomaly C). Within the Plio-Quaternary sedimentary basins, high Vp/Vs anomalies (values higher than 1.9) are observed.

At 4 km depth, small low Vp anomalies are still present beneath the l'Aquila and Fucino basins (anomaly D), while the Vp contrast is reduced beneath the Sulmona basin. Based on seismic reflection profiles and well data, Cavinato et al. (2002) estimated the maximum thickness of the Plio-Quaternary deposits filling the Fucino basin to be

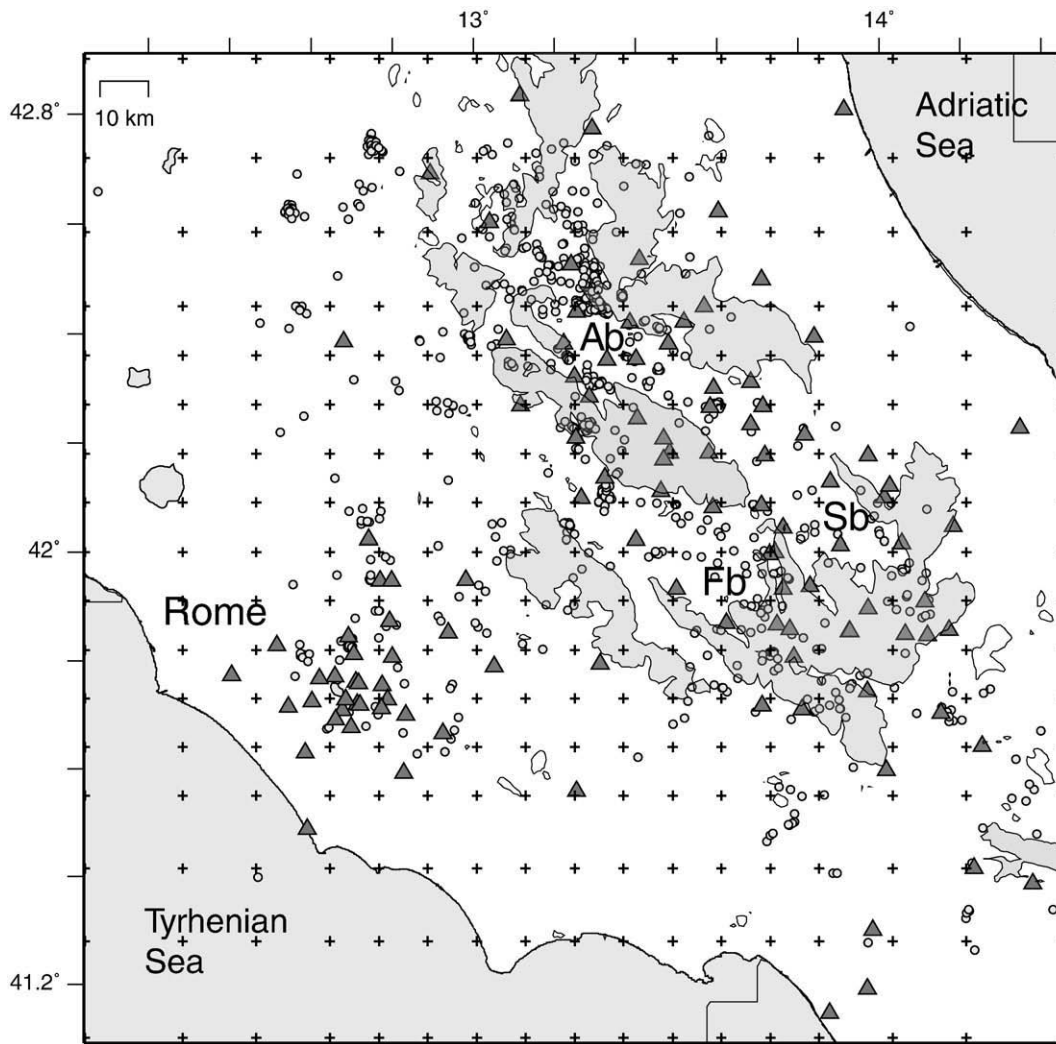


Fig. 3. Seismicity (circles) and seismic stations (triangles) used in the inversion. Crosses are the location of nodes in the velocity model. The gray regions are those with elevation higher than 1000 m. Fb, Sb, and Ab are the Fucino, Sulmona and Aquila basins, respectively.

about 1000 m. The same authors recognize Messinian flysch units, underlying the Plio-Quaternary successions. However, the thickness of the flysch does not exceed 500 m, thus the low velocity anomalies still present at 4 km depth beneath the Plio-Quaternary Fucino and L'Aquila basins may indicate the depression of the limestone basement by the activity of normal faults. A P-wave velocity reduction is observed around the Alban Hills volcano (anomaly E), along with a broad low Vp/Vs anomaly. NNW-trending high Vp anomalies are observed in the central region (6.0–6.5 km/s) beneath the Velino, Sirente and D'Ocre Mts, and to the east beneath the Montagna Grande and Morrone and Montagnone Mts (anomaly B). NNW-trending high Vp/Vs anomalies are predominant beneath the northern and northeastern bounds, whereas minor low Vp/Vs regions are present in the central and southern portions.

At 8 km depth, the dominant features are the NNW-striking high Vp bodies elongated parallel to the central thrust system (anomaly F, in Fig. 4). A second NS-trending high Vp anomaly is observed to the SW of Teramo (anomaly G). The Vp/Vs model reveals positive anomalies beneath the L'Aquila and Fucino basins, surrounded by low Vp/Vs that are also present beneath the Alban Hills and Tyrrhenian regions. The N- and NNE-trending anomalies are located

along the transition zone between the Abruzzi platform and Sabine pelagic basin (Figs. 2 and 4).

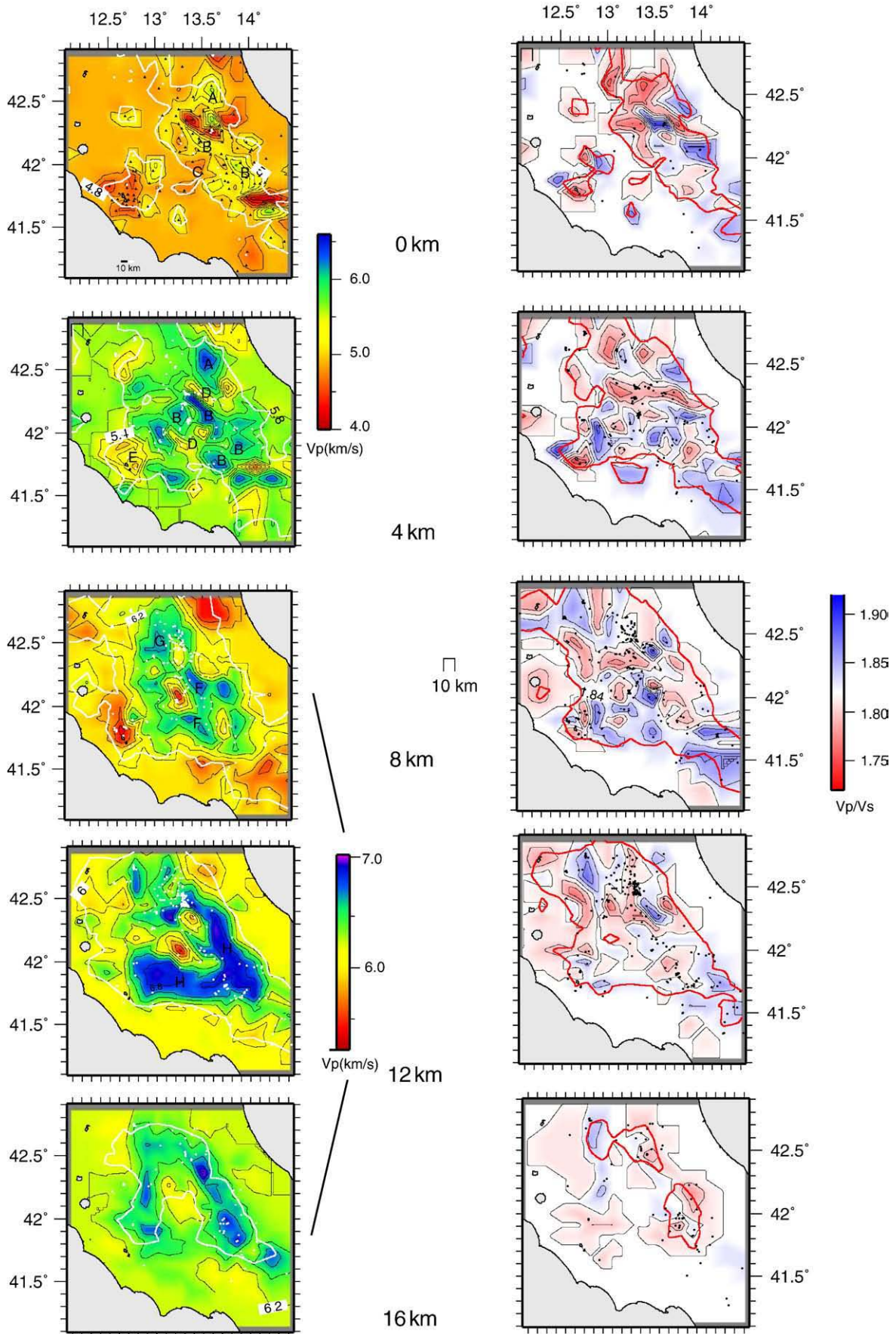
At 12 km depth, two very high Vp anomalies are dominant (Vp in the range 6.7–7.0 km/s). They are located beneath the Simbruini Mts, to the west, and beneath the external front of the Maiella–Gran Sasso thrusts (anomaly H). The two high Vp regions are separated by a low Vp anomaly, located slightly to the west of the Fucino basin. The Vp/Vs model shows a main positive anomaly beneath the L'Aquila basin, and relatively low Vp/Vs values all around.

At 16 km depth, P-wave velocities reach values of about 6.8 km/s that surrounds a central low Vp region. The decrease of low Vp/Vs anomalies seems to be real, but the resolution of both the Vp and Vp/Vs models decreases due to the poor ray sampling.

4. RFs: Data, analysis and modelling

In this study, we used $M_w \geq 5.5$ teleseismic events with epicentral distance between 25° and 100° recorded at three-component stations belonging to the Italian National Network. We computed RFs by deconvolution of the vertical from the radial (R) and transverse (T) horizontal components (see Langston, 1979). RFs are calculated

Fig. 4. P-wave velocity (left) and Vp/Vs (right) layers. The white contour line (red line for the Vp/Vs model) represents the volume comprising the nodes with spread function (SP) ≤ 2 (see the text), i.e. the well resolved volume. White dots (black for Vp/Vs model) are the relocated seismic events.



RRF(Binning 20x40 [BAZxDIST] with 0.5 overlap -- BAZ sweep at epic 70)

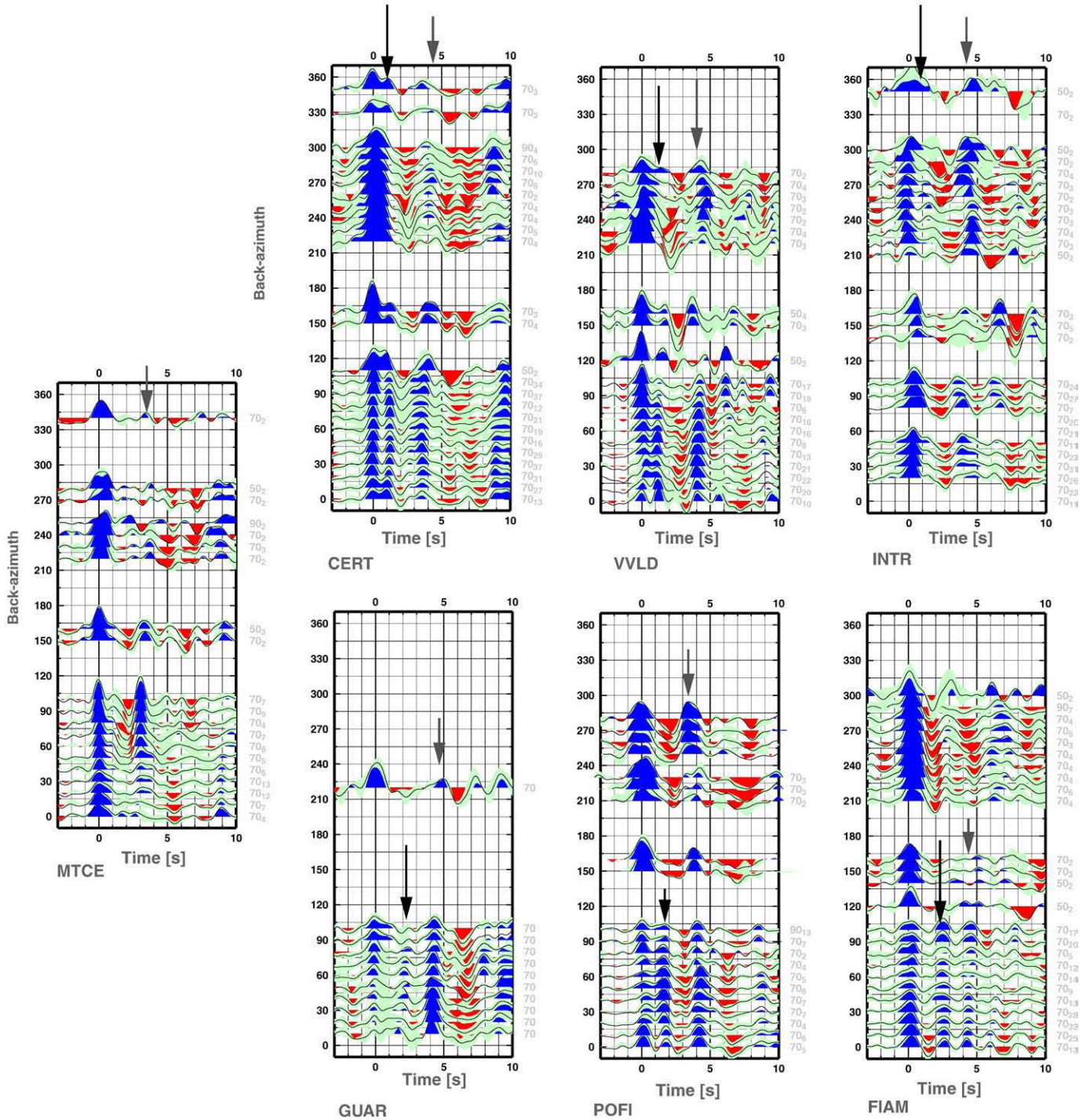


Fig. 5. RFs plotted as a function of back azimuth. Earthquakes with epicentral distance between 70° and 100° are included. The radial components for 7 seismic stations located in the study region show the main features of the data set, such as the top of the high Vs body (black arrow) and the Moho discontinuity (gray arrow).

through a frequency domain deconvolution (Di Bona, 1998) using a Gaussian filter ($\alpha=2$) to limit the final frequency band below about 1 Hz. A better signal-to-noise ratio is achieved by stacking the RFs coming from the same back azimuth direction (ϕ) and epicentral distance (Δ) (Park et al., 2004). Fig. 5 shows the RFs stacked in 50% overlapping bins of back azimuth 20°, and epicentral distance 40°, emphasizing the continuity of the features over the 360° back azimuth, while smoothing high frequency details.

Among our data set (see baz-sweep plot in Fig. 5), we selected two stations (CERT and VVLD) to perform inversions for the Vs model.

Those stations have a consistent number of data and are located on top of the high Vp bodies, therefore can offer independent constrains on the reliability and geometry of the deep features revealed by tomography.

In the recovered data sets, all the back azimuthal directions are evenly sampled, so we can extract the harmonics from the R (and T) data set (shown in Appendix B.). To avoid the doubling of the data set, RFs are stacked in not overlapping bins of 10° in back azimuth and 20° in epicentral distance. Such binning corresponds to a loss of resolution of less than 2 km over 20 km depth.

The harmonics analysis is performed by summation of the components of individual RFs with weight W_{Ri} (and W_{Ti}), dependent on the azimuth (see Farra and Vinnik, 2000, for details). If the RF contains energy in the harmonics, the weighted sum of the R and T should present some homogeneity in the distribution of the signal. We stacked the R and T distribution ($R + T$) to amplify the signal, in case of similarity between R and T (Vinnik et al., 2007). The analysis of $R + T$ diagram is useful to highlight both the isotropic structure and the axis of three-dimensional features (either anisotropic fabric or dipping planes of discontinuities, see also Bianchi et al., 2008).

To model our data, we applied a forward modelling procedure which uses the Neighbourhood Algorithm (NA) to iteratively sample good data-fitting region of an initial parameter space (see for details Sambridge, 1999a,b). Following the original implementation of the NA, we initially generated 1000 samples evenly distributed in the parameter space. From the neighbourhood of the best-fit models, 20 new samples are iteratively re-sampled. After 1000 iterations, we obtained an ensemble of 21,000 models. Synthetic seismograms are computed using the RAYSUM code, which models the propagation of a plane-wave in dipping and/or anisotropic structure (Frederiksen and Bostock 2000).

Among the stations in Fig. 5, those on the belt present a first positive pulse after the P direct arrival with a delay varying between 1 and 2.5 s. For stations CERT and VVLD some robust feature are here described: i) a first positive pulse at a 1 s of delay time, ii) a negative arrival at 2 s (CERT) and at about 3 s (VVLD), and iii) a positive arrival at 4 s (see Fig. 5). These features outline the presence of a high velocity body in the shallow structure at about 7 km depth under CERT and 8 km depth beneath VVLD reaching a V_s of 3.7 and 3.5 km/s respectively. A low velocity jump is present in the middle–lower crust, where the V_s drops to 2.7 and 2.5 at 21 and 19 km depth for the two stations. The Moho arrival is the clear phase shown in Fig. 5 by the gray arrow, at about 4 s delay time, broadly corresponding to a depth of 33 and 28 km for CERT and VVLD. The computed 3D V_s models at both stations are similar and describe the existence of a high V_s body located between 7 and 15 km depth beneath the limestone layer (V_s reaching about 3.7 km/s, anisotropy greater than 6%, see Table A1). See the Appendix B for the discussion of the inversions and retrieved models.

5. Interpretation of the crustal structure

The comparison between laboratory data, seismic reflection data and seismic tomography results in P-wave velocity ranges for rocks composing the upper crust of the Apennines. Plio–Quaternary basin-filling sediments and syn-orogenic sedimentary and flysch (foredeep and thrust-top basins) have P-wave velocities ranging between 2.0 and 3.0 km/s, and 3.4 to 4 km/s respectively, whereas V_p ranging between 5.0 km/s and 6.0 km/s are observed for the Mesozoic carbonates (Bally et al., 1986; Barchi et al., 1998a; Improta et al., 2000). The Triassic Burano formation has the highest P-wave velocity of the sedimentary pile, with values of about 6.3 and 6.7 km/s km/s for the anhydrite and dolomite layers, respectively (e.g. Mostardini and Merlini, 1986; Iannaccone et al., 1998; Barchi et al., 1998a; Trippetta et al., 2008).

While P-wave velocity are mostly influenced by the variation of lithology in the upper crust, the V_p/V_s is more sensible to the different level of cracking in the rocks, pore aspect ratio and fluid pressure and type (Nur, 1972; Zhao and Negishi, 1998; Wang and Nur, 1989; Chiarabba et al., 2009 and references therein). V_p/V_s ratio is useful in discriminating zones saturated with fluids (Nur, 1972), due to the fact that the content and the physical state of fluids affect differently the P- and S-wave velocities.

5.1. The shallow anomalies: 0–8 km depth

The computed V_p model shows significant variations in both horizontal and vertical directions, reflecting a heterogeneous upper crust structure. Although our model parameterization does not allow

imaging the carbonate stack units with the same details of surface geology, a first order correlation between velocity anomalies and surface geology exists. The warping of V_p anomalies follows the main carbonate imbricate sheets. Shallow low V_p velocities (smaller than 4.5 km/s, Fig. 4a) are observed in correspondence with the main Plio–Quaternary basins (Fucino, L'Aquila and Sulmona basins). Since the grid-node vertical spacing is 4 km and the maximum thickness of the basin-filling sediments is expected to be of about 1 km (e.g. Cavinato et al., 2002), the low velocities indicate a significant depression of the limestone units in the central part of the Fucino and L'Aquila basins.

Our model shows significant lateral and vertical V_p/V_s variations within the shallow sedimentary cover. Positive V_p/V_s anomalies are present, both in the shallowest layer and at depth, in correspondence with the Fucino and L'Aquila basins. We interpret such feature as fluid-saturated volumes beneath the Quaternary basins (see geologic evidence in Ghisetti et al., 2001). Low V_p/V_s volumes are observed at 4 and partially at 8 km depth, within the high V_p carbonate sheets (see Fig. 4a), suggesting the presence of fluid under-saturated volumes. The clear low V_p and low V_p/V_s anomalies centred on the Alban Hills volcano can indicate the presence of CO_2 enriched fluids.

5.2. The deep anomalies: 8–16 km depth

The very high P-wave velocity bodies (6.7–7.0 km/s) observed below 8–12 km depth, in a crust volume previously poorly investigated, is the most intriguing result and the assessment of their reliability is crucial. We have performed a synthetic test showing that the extremely high V_p anomalies are well resolved and not artefact of the solution (see the Appendix). The presence of these bodies is independently confirmed by the very sharp picks of converted phases in the first 1–1.5 s of the RF, visible at the two stations located on the high V_p bodies (Fig. 5). The presence of the sharp velocity jump in RF supports the existence of rocks with velocity higher than limestones underneath the Mesozoic sedimentary pile. The RF inversions show that the S-wave velocities underneath the topmost limestone layer are in the range of 3.6–3.8 km/s, consistent with those defined by the tomographic model. The shift of the picks, visible in the baz-sweep plots, are consistently resolved in the inversion by dipping planes of the high V_s layer, whose trend and plunge agree with the shape of the velocity anomaly in tomograms (Figs. 6 and 7), once more confirming the reliability of the feature.

All the rocks outcropping or drilled in the Apennines has a P-wave velocity smaller than 6.7 km/s, being the Triassic evaporitic layer the fastest (see results for the Alessandra1 well in northern Apennines; A.G.I.P. S.p.A.). The observed V_p range (6.7–7.0 km/s) is inconsistent with sedimentary rocks.

At the same mid-crustal depth, local deep seismic reflectors are observed in the CROP11 profile and are interpreted either as a deep anticlinorium (Billi et al., 2006) or indistinct Permo–Triassic sedimentary sequences (Patacca et al., 2008). Billi and Tiberti (2009) modelled a negative Bouguer anomaly, found in correspondence of the deep anticlinorium and of our velocity jump, as due to a low-density body (2.57 g/cm^3). In both interpretations, these units are involved in the compression that formed the belt.

Similar high V_p bodies have been identified underneath the southern Apennines and ascribed either to crystalline rocks (Chiarabba and Amato, 1997; Bisio et al., 2004; Improta and Corciulo, 2006) or to dolomitic rocks (Iannaccone et al., 1998; Improta et al., 2000). The high V_p and high V_s values found in this work are incompatible with sedimentary or low-grade metamorphic rocks, whilst they might be consistent with the highest values ever observed for dolomitic rocks (Faccenda et al., 2007; De Paola et al., 2008). Dolomites rocks may fill ultra-thickened Triassic syntectonic basins in the hanging wall of normal faults formed during Permo–Triassic rift episodes. Anyway, the thickness for these deposits (4–6 km) is probably too high if compared with other regions of the Adria passive margin (Barchi et al., 1998a,b)

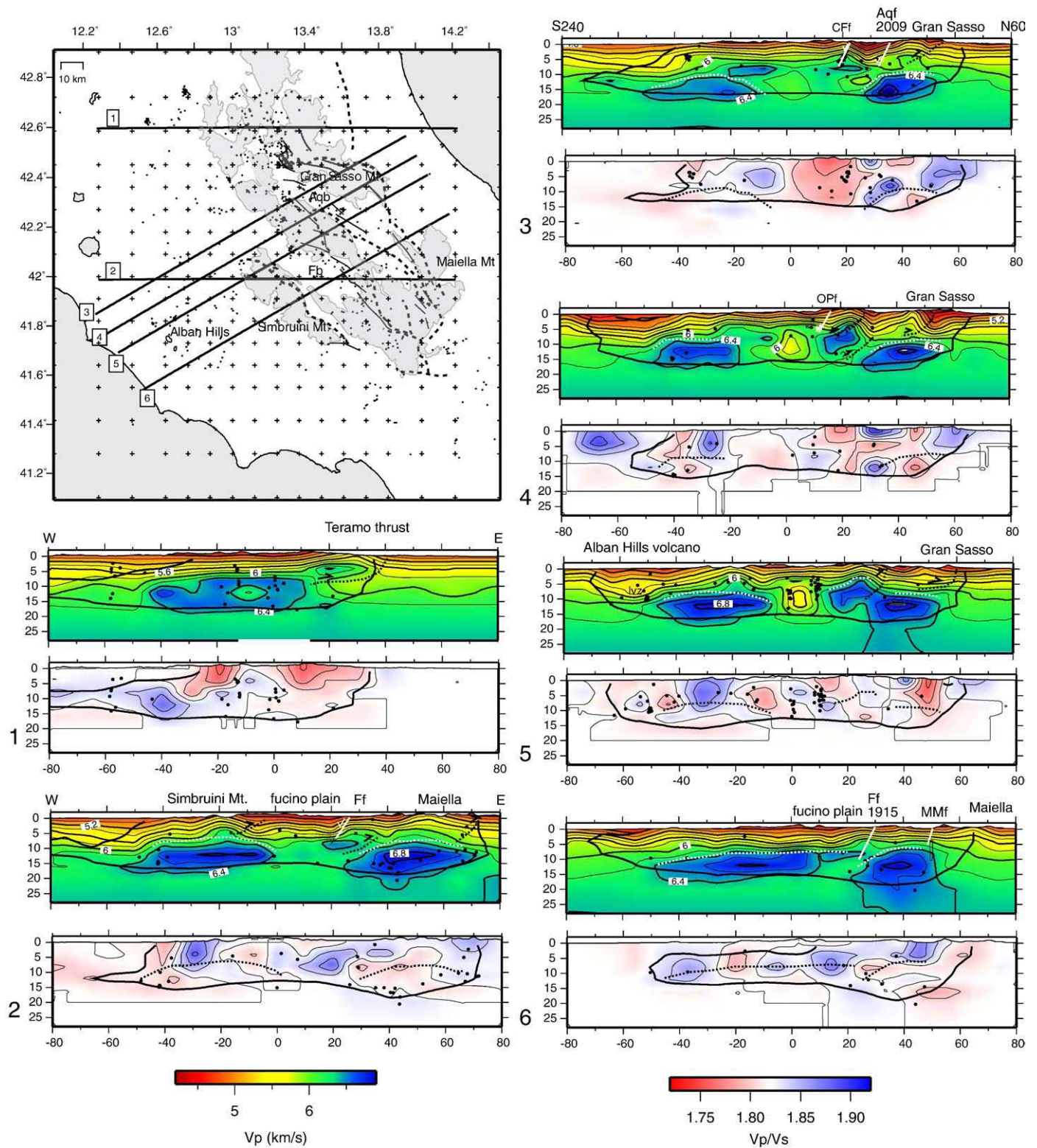


Fig. 6. Vp and Vp/Vs model vertical sections along with the relocated seismicity. Section 2 is almost coincident with the CROP11 profile. The normal faults were drawn based on the surface trace and an average dip of 60° (Mostardini and Merlini, 1986; Pantosti et al., 1996; Piccardi et al., 1999; Barchi et al., 2000; Galadini and Galli, 2000; Palombo et al., 2004; Papanicolaou et al. 2005 among others, see Fig. 2 for names and position of the normal faults, Aqf is the 2009 ruptured fault). The black lines define the well-resolved area of Vp and Vp/Vs models. The white (for the Vp model) and black (for the Vp/Vs model) dashed lines represent the top of the high Vp bodies (coincident with the discontinuity modelled in the receiver functions, see Fig. 7). Dashed black lines in the Vp sections (and gray lines in the map) are the main thrusts.

and its depth requires that the overlaying sedimentary cover be almost doubled. Moreover, the exceptionally high velocities are not observed by seismic tomography and RFs in the northern Apennines, where the

Triassic formations are widely present in the substratum (Barchi et al., 1998a,b) and have a P-wave velocity only slightly higher than 6.2 km/s (Chiarabba et al., 2009).

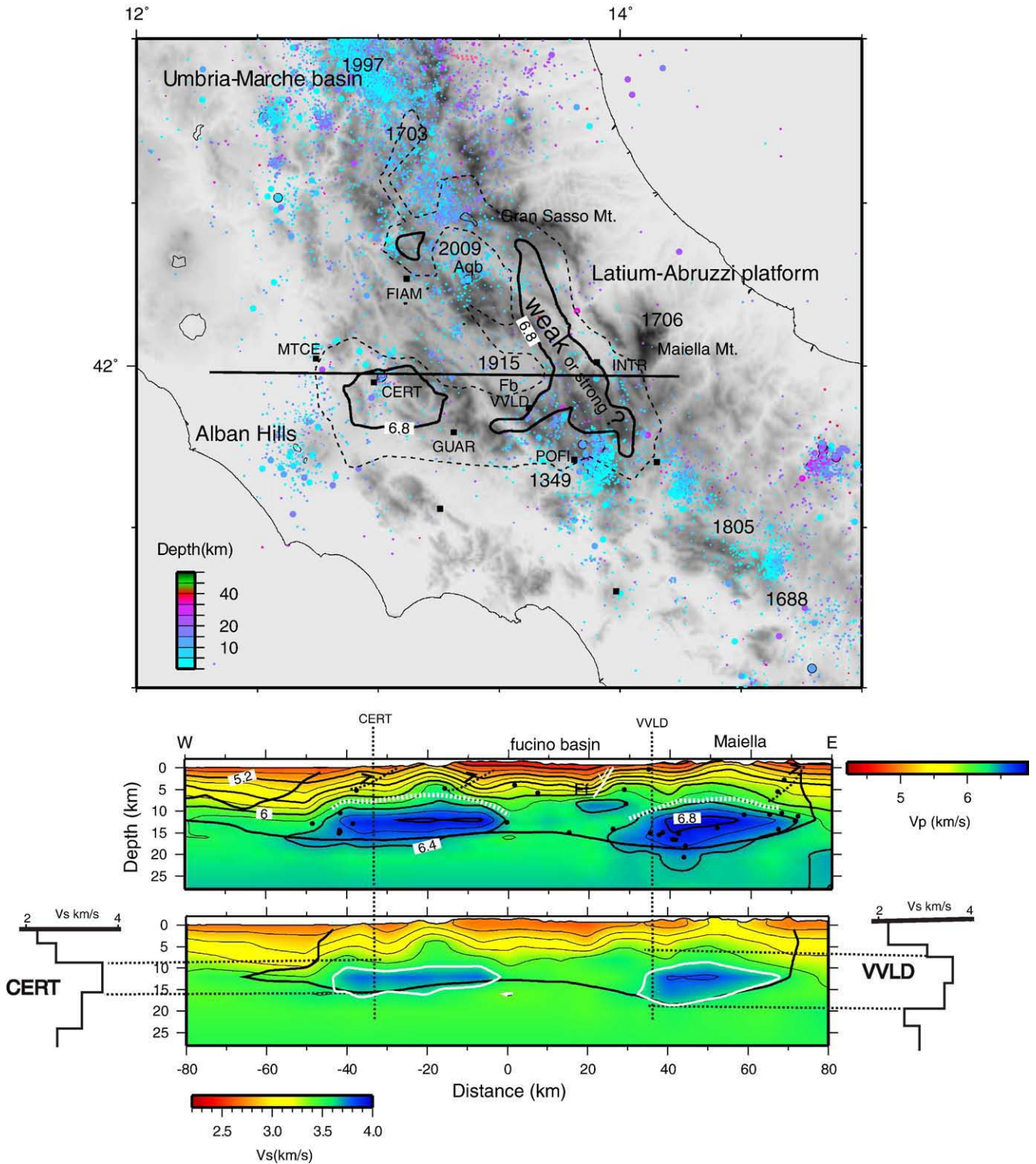


Fig. 7. Map showing the instrumental seismicity of the past 28 years in central Apennines. Moderate magnitude and background seismicity occur around the high Vp, high Vs bodies, outlined by the Vp isoline of 6.8 km/s at 12 km depth (thick black line). Fb and Aqb indicate the Fucino and L'Aquila basin. The dates of the most recent large earthquake occurring on the normal fault system are reported on the map. The black squares are the permanent seismic stations used in the RF analysis. The bold line is the trace of the vertical section, shown in the lower panel. In the section through the Vp model (top), the white dashed contour indicates the top of the high Vp body. The lower section shows the Vs model obtained by the Vp and Vp/Vs models compared with the 1D Vs model for the inversion of RF at stations CERT and VVLD. The white line is the isoline of 3.6 km/s. Note the good correspondence between Vs values from tomography and RF.

Alternatively, they may be explained by deep crustal or mantle rocks exhumed before the sedimentation of the Mesozoic cover. Due to the positive magnetic anomaly observed in the same area (Chiappini et al., 2000; Speranza and Chiappini, 2002), the absence of positive Bouguer anomalies (Tiberti et al., 2005) required for

dolomitic or deep crustal granulitic rocks (density as high as than 2.86 g/cm³), the anisotropy greater than 6%, the reflectivity observed in the CROP11 seismic line (Patacca et al., 2008), and the thickness and continuity of this layer, the interpretation of these anomalies as originated by hydrated mantle rocks such as serpentines seems to be

more reliable. P- and S-wave velocities, S-wave anisotropy (>6%) and density values could be consistent with a percentage of serpentine of about 30% (see Horen et al., 1996).

5.3. The sub-surface structure from vertical sections across the belt

The high Vp anomalies show the lateral extent of the limestone units forming the bulk of the central Apennines belt. Vertical sections across the belt (Fig. 6) show that the uppermost crust is dominated by strong lateral heterogeneities that define the thrusting of the Mesozoic cover. The deep high Vp and high Vs bodies are also involved in thrusting.

Section 1 (Fig. 6) shows a very clear high Vp anomaly that coincides with the Montagnone Mt. anticline developed on the Teramo thrust that is decolled at shallow depth. Background seismicity is absent on this thrust. This N–S elongated structure is well visible in tomograms in the northern part of the area.

Section 2, running almost along the CROP11 seismic profile, shows two main high Vp thrust units, the Simbruini Mts. and the Maiella thrusts to the west and east, respectively. Both thrusts are rooted in the high Vp, high Vs anomalies at depth. The Fucino plain is characterized by negative velocity anomalies down to 4 km depth, and the Fucino normal fault (Ff), responsible for the 1915 Avezzano earthquake, is visible as a gentle warping of anomalies in the eastern border of the basin. The 5.2 km/s isoline (see Section 2) defines a lateral step in the limestone units compatible with the presence of a normal fault along which repeated earthquakes form the Quaternary basin. Background seismicity is almost absent on this fault segment, suggesting that the fault is completely locked during the interseismic period started about 100 years ago. In the mid-crust, the high Vp bodies are the most prominent feature, the westernmost one associated with mid-crustal reflectors in the CROP11 seismic profiles interpreted as a deep antiformal unit (Billi et al., 2006). The easternmost body is located beneath the Maiella thrust, connected with structures and faults in the uppermost crust.

Sections 3 to 5 are drawn perpendicularly to the Apennines structures and reveal, from north to south, the geometry of the thrusts. In Sections 3 and 4, the two main thrust units of the Mt. Ocre and Gran Sasso are strikingly imaged. Thrusts units are composed by the entire Mesozoic sediments pile from the Triassic evaporitic rocks (Vp higher than 6.2 km/s) to the limestone and basin terrigenous facies (Vp between 4.2 to 6 km/s). In between them, the L'Aquila basin is defined by a consistent decrease of Vp down to 4 km depth. In Section 5, the westernmost Mt. Simbruini thrust is visible, involving the deep high Vp body. To the west of this unit, a low Vp anomaly marks the Tyrrhenian region and surrounds the Quaternary Alban Hill volcano.

The overall geometry is that of shallow high velocity limestone rocks forming anticlines developing on E- to NE-ward trending, following two main systems visible at the surface (see the structural sketch in Fig. 2). The two main systems along the arc-shape belt are replicated at depths by the very high Vp, high Vs bodies. The total displacement of the external thrust system (Gran Sasso–Ocre–Maiella) inferred by tomographic images is generally lower than 10 km, except the Teramo thrust that reaches the largest values of about 10–15 km.

Low Vp and high Vp/Vs regions are found beneath the L'Aquila and Fucino Quaternary basins (between 4 and 12 km depth), suggesting the existence of fluid-saturated rock volumes.

6. Discussions

In this section, we describe how our new results contribute to the understanding of both seismicity occurrence, furnishing a readable perspective of the L'Aquila 2009 earthquake, and tectonic style of the

continental collision belt of central Apennines. The close match between tomographic and RF results gives a significant validation to the main, original feature revealed at mid-crustal depth: the ultra-speed body underneath the Mesozoic sedimentary cover (Fig. 7).

6.1. Relation between the sub-surface structure and seismicity

The relocated seismicity is sparsely distributed and does not clearly align on the Quaternary faults (Figs. 6 and 7). The main normal faults of the area, presumably responsible for historical earthquakes, do not show significant seismic activity in the examined period (see also Bagh et al. 2007). Background seismicity with magnitude down to $M_L 1.0$ occurs either sparsely in the area or in few and small clusters not clearly connected with faults. Very strikingly, none of the earthquakes occurred in the past 30 years (CSI catalogue, Chiarabba et al., 2005) within the high-speed bodies located in the mid-crust (Fig. 7).

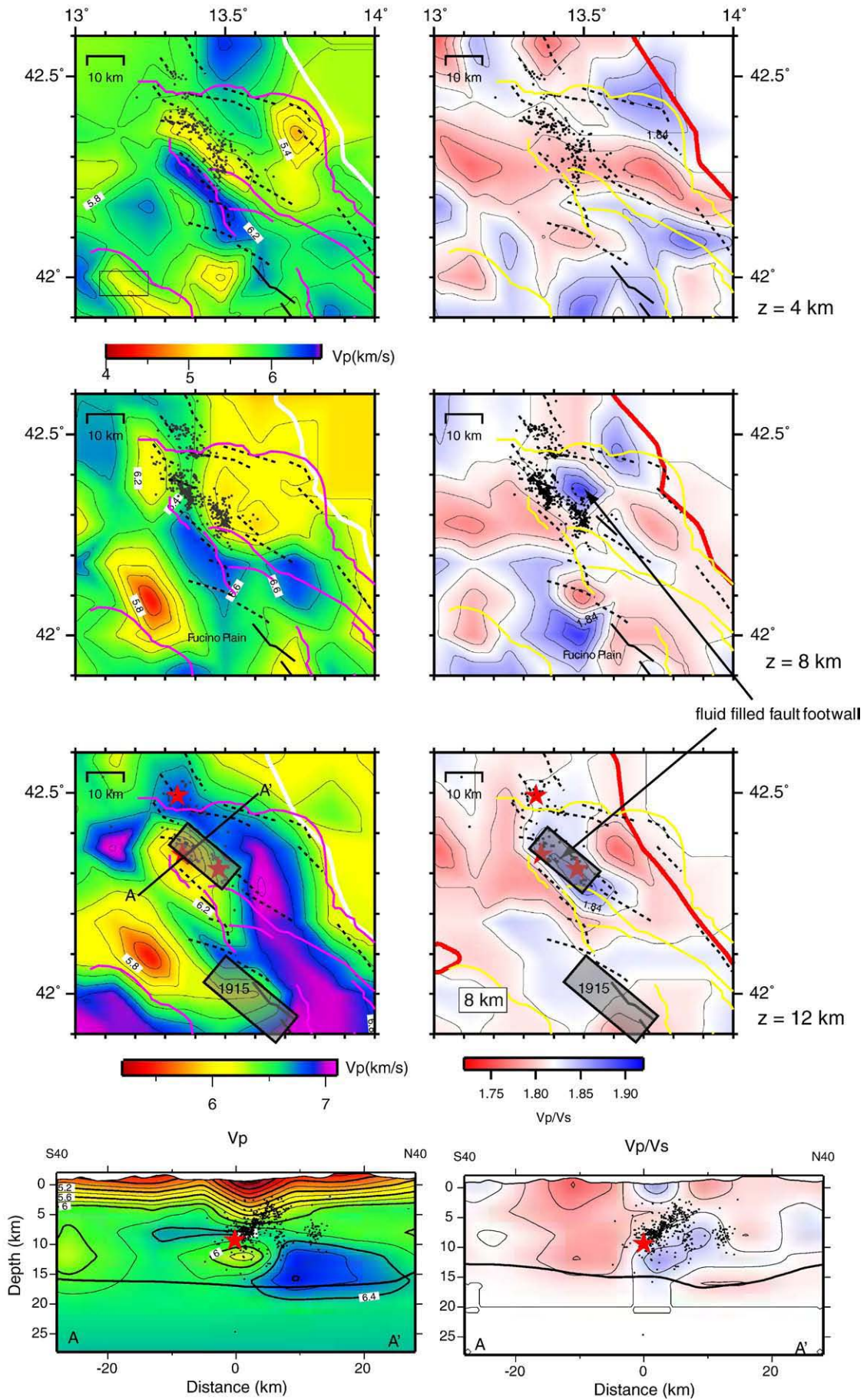
The role played by the high velocity bodies in controlling seismicity occurrence and deformation is difficult to be assessed and open two opposite hypotheses. They might be strong blocks and act as asperities slipping with large earthquakes. In the literature, high velocity zones along faults were related to high-strength regions where large stress drops and relatively large slip occur (e.g. Scholz, 1990; Zhao and Kanamori, 1992; Chiarabba and Selvaggi, 1997; Chiarabba and Amato, 2003). We remind that the interpretation of the high Vp, high Vs bodies in terms of dolomitic rocks is consistent with this scenario, since the very brittle nature of dolomites (De Paola et al., 2008). Oppositely, they can be weak and distribute the deformation in a ductile regime. The interpretation of the high-speed bodies in terms of serpentines rocks is more consistent with this weak behavior (Escartin et al., 1997; Reinen, 2000). The absence of instrumental seismicity within these bodies (Fig. 7) may be a further evidence for this hypothesis. In this case, the active normal faults develop only at the border of the high-speed bodies, or above them, resulting in small segments decolled at 6–8 km depth. The friction response of hydrated mafic rocks, such as serpentines, strongly depends on the loading slip velocity. A velocity strengthening response inhibits the unstable behavior either for small and constant loading velocities or at greater depths for the concomitant effect of pressure (see Reinen et al., 1991; Escartin et al., 1997). In our case, the absence of historical earthquakes in the past 0.8 ka clearly associated to faults located within these bodies (CPTI working group) and the extensional deformation rate observed by recent geodetic studies, in the order of a few mm/yr (Hunstad and England, 1999; D'Agostino et al., 2008), may favor the latter interpretation. Therefore, the extensional deformation in central Apennines may be predominantly accommodated by the faults in the Fucino and L'Aquila basins, those ruptured by the two most recent destructive earthquakes.

6.2. The 2009 L'Aquila sequence

Although our understanding of this sequence is obviously incomplete and still in progress, some striking features are observed. Fig. 8 shows the location of the three $M_L > 5$ events of the sequence (Chiarabba et al., 2009) and the relocation of aftershocks done using the routinely picked P- and S-wave arrivals of the seismic network (by heterogeneous analysts during the h24 surveillance service) with the 3D velocity model.

The mainshock hypocenter is located at around 10 km depth in a low Vp high Vp/Vs volume. The aftershocks define a main SW-dipping plane located on top of a high Vp/Vs volume (see the vertical section in Fig. 8). We interpret the low Vp, high Vp/Vs anomalies as a fluid filled volume already present in the footwall of the fault some years

Fig. 8. Zoom of the Vp and Vp/Vs models on the L'Aquila region. The mainshock, aftershocks and tentative fault geometry are shown on the layers. The large square in the bottom layer is the normal fault ruptured by the 1915 Avezzano earthquake. We note a high Vp/Vs low Vp anomaly in the footwall of the L'Aquila fault, which extent nicely match that of the activated fault portion.



before the 2009 event (at least during 2003–2004). Such observation emphasizes the role of fluids in earthquake generation. Based on the extent of the high Vp/Vs anomaly at 8–12 km depth (see Fig. 8), larger than the fault ruptured by the 6th of April main event fault, there is probably a southern extension of the fault with a fluid-filled volume in the footwall. The main fault and aftershocks are almost completely confined by the mid-crustal high-speed bodies, southward. From the tomographic results, the only two areas with low Vp and high Vp/Vs anomalies in the upper crust are the Fucino and the L'Aquila basins, i.e. the two areas where destructive earthquakes occurred in the past 100 years.

6.3. Tectonic style of the central Apennines

Until now, the formation of the Apennines belt has been explained adopting thin- or thick-skinned tectonic models (Coward, 1983; Bally et al., 1986; Mostardini and Merlini, 1986; Hill and Hayward, 1988; Roure et al., 1991; Ghisetti et al., 1993; Tozer et al., 2002; Butler et al., 2004; Scrocca et al., 2005). Thin-skinned models assume that the carbonate Mesozoic cover is decolled from a mostly un-deformed Paleozoic basement, presumably along the Triassic evaporitic layer. This requires the subduction of the continental lithosphere that seems to be ceased in central Apennines some My ago, as indicated by the absence of both high Vp slab in the uppermost mantle (Lucente et al., 1999; Piromallo and Morelli, 2003) and intermediate depth seismicity (Chiarabba et al., 2005).

Our main finding is the presence of exceptionally high Vp and Vs bodies in the middle crust whose geometry follows that of the belt at the surface, following the Gran Sasso and Maiella thrust systems (Fig. 7). These bodies influenced the evolution of the belt, resulting in a tectonic model that has either thin-skinned or thick-skinned features. The displacement of major thrusts, inferred by tomographic models, is smaller than 10–15 km on average, in agreement with the geologic results by Mazzoli et al. (2005). We do not find evidence that the Triassic evaporitic sequence act as the main decollement, but the high velocity bodies are involved in thrusting. The interpretation in terms of dolomitic rocks preferentially supports this conclusion and suggests that, during Plio-Pleistocene, thrusts reactivate the Mesozoic normal faults previously bounding the basins where dolomitic rocks were deposited (Fig. 6).

The alternative interpretation, i.e., a laterally heterogeneous Paleozoic basement, is tantalizing. It could imply that the continental margin of the Tethys was strongly stretched and portions of the hydrated mantle exhumed before the sedimentation of the Mesozoic cover. This hypothesis agrees with analogic experiments that model the stretching of continental crust (Brun and Beslier, 1996) and with geologic evidence of deep exhumation of serpentines underneath the sedimentary cover of Pyrenees (Lagabrielle and Bodinier, 2008) and along the ocean-continent corridor Alpine Tethys (Manatschal and Muntener, 2008). Other geophysical data, ad hoc gravimetric and magnetic surveys, could provide independent constraints on which of the two hypotheses is the more likely.

7. Conclusions

Seismic tomography and receiver functions yield new, independent and consistent information on the upper-middle crust of the Abruzzi region in central Apennines. We find the existence of very high Vp and Vs bodies in the mid-crust that can be ascribed to either a very thick layer of dolostones or hydrated mafic rocks. This latter hypothesis implies the presence of a laterally heterogeneous Paleozoic basement derived from the thinning of the Tethys continental margin and exhumation of hydrated mantle rocks. Although the interpretation is speculative, our results may open a debate on how the continental margins are thinned during the first stage of the extension.

The past years seismicity and large magnitude earthquakes (Fucino 1915 and L'Aquila 2009) occur at the border of these high velocity bodies, suggesting that the rheology of this material influence the development of the Apennines belt and are today controlling the segmentation of the active normal fault system. Both the Fucino and L'Aquila areas feature a shallow low Vp sedimentary basin and deep low Vp and high Vp/Vs anomalies in the fault footwall, consistent with the presence of fluid-filled rock volumes. It is striking that only in those two areas we identify low Vp and high Vp/Vs anomalies at seismogenic depths. Such features were also visible some years before the 2009 event, but unfortunately not easily explainable before the earthquake.

Acknowledgement

We thank the editor and the two anonymous reviewers for giving some significant suggestions for the improvement of our paper. We also thank A. Amato, C. Faccenna, A. Billi and F. Speranza for helpful discussion. IB is supported by DPC-S1_UR02.02. We used GMT software (Wessel and Smith, 1991) to prepare figures.

Appendix A. Supplementary data

Supplementary data associated with this article can be found, in the online version, at doi:10.1016/j.epsl.2010.04.028.

References

- Amoruso, A., Crescentini, L., Scarpa, R., 1998. Inversion of source parameters from near and far field observations: an application to the 1915 Fucino earthquakes, central Apennines. *J. Geophys. Res.* 103, 29,989–29,999.
- Atzori, S., Hunstad, I., Chini, M., Salvi, S., Tolomei, C., Bignami, C., Stramondo, S., Trasatti, E., Antonioli, A., Boschi, E., 2009. Finite fault inversion of DInSAR coseismic displacement of the 2009 L'Aquila earthquake (central Italy). *Geophys. Res. Lett.* 36, L15305. doi:10.1029/2009GL039293.
- Bagh, S., Chiaraluce, L., De Gori, P., Moretti, M., Govoni, A., Chiarabba, C., Di Bartolomeo, P., Romanelli, M., 2007. Background seismicity in the Central Apennines of Italy: the Abruzzo region case study. *Tectonophysics* 444, 80–92.
- Bally, A.W., Burbi, L., Cooper, C., Ghelardoni, R., 1986. Balanced sections and seismic reflection profiles across the central Apennines. *Mem. Soc. Geol. Ital.* 35, 257–310.
- Barchi, M., De Feyter, A., Magnani, B., Minelli, G., Piali, G., Sotera, B.M., 1998b. The structural style of Umbria–Marche fold and thrust belt. *Mem. Soc. Geol. Ital.* 111, 557–578.
- Barchi, M., Minelli, G., Piali, G., 1998a. the CROP03 profile: a synthesis of results on deep structures of the northern Apennines. *Mem. Soc. Geol. Ital.* 52, 383–400.
- Barchi, M., Galadini, F., Lavecchia, G., Messina, P., Michetti, M., Peruzza, L., Pizzi, A., Tondi, E., Vittori, E., 2000. Sintesi delle conoscenze sulle faglie attive in Italia centrale: parametrizzazione ai fini della caratterizzazione della pericolosità sismica. Report for CNR – Gruppo Nazionale per la Difesa dai Terremoti (GNDT).
- Bianchi, I., Piana Agostinetti, N., De Gori, P., Chiarabba, C., 2008. Deep structure of the Colli Albani volcanic district (central Italy) from receiver functions analysis. *J. Geophys. Res.* 113, B09313. doi:10.1029/2007JB000548.
- Bigi, S., Pisani, P.C., 2005. From a deformed peri-Tethyan carbonate platform to a fold-and-thrust-belt: an example from the Central Apennines (Italy). *J. Struct. Geol.* 27, 523–539.
- Billi, A., Tiberti, M.M., 2009. Possible causes of arc development in the Apennines, central Italy. *GSA Bull.* doi:10.1130/B26335.1
- Billi, A., Tiberti, M.M., Cavinato, G.P., Cosentino, D., Di Luzio, E., Keller, J.V.A., Kluth, C., Orlando, L., Parotto, M., Praturion, A., Romanelli, M., Storti, F., Wardell, N., 2006. First results from the CROP-11 deep seismic profile, central Apennines, Italy: evidence of mid-crustal folding. *J. Geol. Soc. Lond.* 163, 583–586.
- Bisio, L., Giovambattista, R.D., Milano, G., Chiarabba, C., 2004. Three-dimensional earthquake locations and upper crustal structure of the Sannio-Matese region (southern Italy). *Tectonophysics* 385, 121–136.
- Boncio, P., Lavecchia, G., Pace, B., 2004. Defining a model of 3D seismogenic sources for Seismic Hazard Assessment applications: the case of central Apennines (Italy). *J. Seismol.* 8, 407–425. doi:10.1023/B:JOSE.0000038449.78801.05.
- Brun, J.P., Beslier, M.O., 1996. Mantle exhumation at passive margins. *Earth Planet. Sci. Lett.* 112, 161–173.
- Butler, R.W.H., Mazzoli, S., Corrado, S., De Donatis, M., Di Bucci, D., Gambini, R., Nasp, G., Vicoli, C., Scrocca, D., Shiner, P., Zucconi, V., 2004. Applying thick-skinned tectonic model to the Apennine thrust-belt of Italy: limitations and implications. In: McClay, K.R. (Ed.), *Thrust Tectonic and hydrocarbon system*: American Association of Petroleum Geologists Memoir, 82, pp. 647–667.
- Calamita, F., Deiana, G., 1988. The arcuate shape of the Umbria–Marche–Sabina Apennines (Central Italy). *Tectonophysics* 146, 139–147.

- Calamita, F., Paltrinieri, W., Pelorosso, M., Scisciani, V., Tavarnelli, A., 2003. Inherited mesozoic architecture of the Adria continental palaeomargin in the Neogene central Apennines orogenic system, Italy. *Boll. Soc. Geol. Ital.* 122, 307–318.
- Calamita, F., Viandante, M.G., Hegarty, K., 2004. Pliocene-Quaternary burial/exhumation paths of the central Apennines (Italy): implications for the definition of the deep structure of the belt. *Boll. Soc. Geol. Ital.* 123, 503–512.
- Castellarin, A., Colacicchi, R., Praturion, A., Cantelli, C., 1982. The Jurassic-Lower Pliocene history of Ancona–Anzio line (central Italy). *Mem. Soc. Geol. It.* 24, 325–336.
- Cavinato, G.P., De Celles, P.G., 1999. Extensional basins in the tectonically bimodal central Apennines fold-thrust belt, Italy: response to corner flow above subducting slab retrograde motion. *Geology* 27, 955–958.
- Cavinato, G.P., Carusi, C., Dall'Asta, M., Miccadei, E., Piacentini, T., 2002. Sedimentary and tectonic evolution of Plio-Pleistocene alluvial and lacustrine deposits of Fucino basin (central Italy). *Sediment. Geol.* 148, 29–59.
- Chiappini, M., Meloni, A., Boschi, E., Faggioni, O., Beverini, N., Carmisciano, C., Marson, I., 2000. Shaded relief magnetic anomaly map of Italy and surrounding marine areas. *Ann. Geofis.* 43, 983–989.
- Chiarabba, C., Amato, A., 1997. Upper-crustal structure of the Benevento area (southern Italy): fault heterogeneities and potential for large earthquakes. *Geophys. J. Int.* 130, 229–239.
- Chiarabba, C., Amato, A., 2003. Vp and Vp/Vs images in the M_w 6.0 Colfiorito fault region (central Italy): a contribution to the understanding of seismotectonic and seismicogenic processes. *J. Geophys. Res.* 108. doi:10.1029/2001JB001665.
- Chiarabba, C., Selvaggi, G., 1997. Structural control on fault geometry: the example of the Grevena M_s 6.6 normal faulting earthquake. *J. Geophys. Res.* 102, 22445–22457.
- Chiarabba, C., Jovane, L., Di Stefano, R., 2005. A new look to the Italian seismicity: seismotectonic inference. *Tectonophysics* 395, 251–268.
- Chiarabba, C., et al., 2009. The 2009 L'Aquila (central Italy) MW6.3 earthquake: Main shock and aftershocks. *Geophys. Res. Lett.* 36, L18308. doi:10.1029/2009GL039627.
- Coward, M.P., 1983. Thrust tectonics, thin skinned or thick skinned, and the continuation of thrusts to deep in the crust. *J. Struct. Geol.* 5, 113–123.
- D'Agostino, N., Giuliani, R., Mattone, M., Bonci, L., 2001. Active crustal extension in the central Apennines (Italy) inferred from GPS measurements in the interval 1994–1999. *Geophys. Res. Lett.* 28, 2121–2124.
- D'Agostino, N., Avallone, A., Cheloni, D., D'Anastasio, E., Mantenuto, S., Selvaggi, G., 2008. Active tectonics of the Adriatic region from GPS and earthquake slip vectors. *J. Geophys. Res.* 113. doi:10.1029/2008JB005860.
- D'Addezio, G., Masana, E., Pantosti, D., 2002. The Holocene paleoseismicity of the Aremogna-Cinque Miglia fault (Central Italy). *J. Seismol.* 5, 181–205.
- De Luca, G., Cattaneo, M., Monachesi, G., Amato, A., 2009. Seismicity in Central and Northern Apennines integrating the Italian national and regional networks. *Tectonophysics*. doi:10.1016/j.tecto.2008.11.
- De Paola, N., Collettini, C., Faulkner, D.R., Trippetta, F., 2008. Fault zone architecture and deformation processes within evaporitic rocks in the upper crust. *Tectonics* 27, TC4017. doi:10.1029/2007TC002230.
- Decandia, F.A., Lazzaretto, A., Lotta, D., Cernobori, L., Nicolich, R., 1998. The CROP 03 traverse: insights on postcollisional evolution of the Northern Apennines. *Mem. Soc. Geol. Ital.* 52, 427–439.
- Decandia, F.A., Tavernelli, E., Alberti, M., 2002. La doppia riattivazione della linea della Valnerina: implicazioni per l'evoluzione tettonica dell'Appennino Umbro Marchigiano. *Studi Geol. Camerti* 1, 77–86.
- Di Bona, M., 1998. Variance estimate in frequency-domain deconvolution for teleseismic receiver function computation. *Geophys. J. Int.* 134, 634–646.
- Di Stefano, R., Kissling, E., Chiarabba, C., Amato, A., Giardini, D., 2009. Shallow subduction beneath Italy: three-dimensional images of the Adriatic-European-Tyrrhenian lithosphere system based on high-quality P wave arrival times. *J. Geophys. Res.* 114, B05305. doi:10.1029/2008JB005641.
- Dondi, L., Papetti, I., Tedeschi, D., 1966. Stratigrafia del pozzo Trevi 1 (Lazio). *Geol. Rom.* pp. 249–262.
- Eberhart-Phillips, D., 1993. Local earthquake tomography: earthquake source region. In: Iyer, H.M., Hirahara, K.K. (Eds.), *Seismic Tomography: Theory and Practice*, pp. 613–643. New York.
- Eberhart-Phillips, D., Reyners, M., 1997. Continental subduction and three-dimensional crustal structure: the Northern South Island New Zealand. *J. Geophys. Res.* 102, 11843–11861.
- Elter, P., Ciglia, G., Tongiorgi, M., Trevisan, L., 1975. Tensional and compressional areas in the recent (Tortonian to present) evolution of the northern Apennines. *Boll. Geofis. Teor. Appl.* 17, 3–18.
- Escartin, J., Hirth, G., Evans, B., 1997. Nondilatant brittle deformation of serpentinites: implications for Mohr–Coulomb theory and the strength of faults. *J. Geophys. Res.* 102, 2897–2913.
- Faccenda, M., Bressan, G., Burlini, L., 2007. Seismic properties of the upper crust in the central Friuli area (northeastern Italy) based on petrophysical data. *Tectonophysics* 445, 210–226.
- Farra, V., Vinnik, L., 2000. Upper mantle stratification by P and S receiver functions. *Geophys. J. Int.* 141 (3), 699–712.
- Frederiksen, A.W., Bostock, M.G., 2000. Modeling teleseismic waves in dipping anisotropic structures. *Geophys. J. Int.* 141, 401–412.
- Frepoli, A., Amato, A., 1997. Contemporaneous extension and compression in the northern Apennines from earthquake fault-plane solutions. *Geophys. J. Int.* 129, 368–388.
- Galadini, F., Galli, P., 1999. The Holocene paleoearthquakes on the 1915 Avezzano earthquake faults (central Italy): implications for active tectonics in the central Apennines. *Tectonophysics* 308, 143–170.
- Galadini, F., Galli, P., 2000. Active tectonics in the central Apennines (Italy) – input data for seismic hazard assessment. *Nat. Hazards* 22, 225–270.
- Ghisetti, F., Vezzani, L., 1997. Geometrie deformative ed evoluzione cinematica dell'Appennino Centrale. *Stud. Geol. Camerti* XIV, 127–154.
- Ghisetti, F., Barchi, M., Bally, A.W., Moretti, I., Vezzani, L., 1993. Conflicting balanced structural sections across the central Apennines (Italy): problems and implications. In: Spencer, A.M. (Ed.), *Generation, accumulation and production of Europe's hydrocarbons, III: Heidelberg, Springer-Verlag, European Association of Petroleum Geologists, Special Publication n. 3*, pp. 219–231.
- Ghisetti, F., Kirschner, D., Vezzani, L., Agosta, F., 2001. Stable isotope evidence for contrasting paleofluid circulation in thrust faults and normal faults of the central Apennines, Italy. *J. Geophys. Res.* 106, 8811–8825.
- Hill, K.C., Hayward, A.B., 1988. Structural constraints on the Tertiary plate tectonic evolution of Italy. *Marine and Petroleum Geology* 5, 2–16.
- Horen, H., Zamora, M., Dubuisson, G., 1996. Seismic waves velocities and anisotropy in serpentinized peridotites from Xigaze ophiolite: abundance of serpentine in slow spreading ridge. *Geophys. Res. Lett.* 23, 9–12.
- Hunstad, I., England, P., 1999. An upper bound on the rate of strain in the central Apennines, Italy, from triangulation measurements between 1869 and 1963. *EPSL* 169, 261–267.
- Iannaccone, G., Improta, L., Capuano, P., Zollo, A., Biella, G., De Franco, R., Deshamps, A., Cocco, M., Mirabile, L., Romeo, R., 1998. A P-wave velocity model of the upper crust of the Sannio region (Southern Apennines, Italy). *Ann. Geofis.* 41 (4), 567–582.
- Improta, L., Corciulo, M., 2006. Controlled source non-linear tomography: a powerful tool to constrain tectonic models of the southern Apennines orogenic wedge, Italy. *Geology* 34 (11), 941–944.
- Improta, L., Iannaccone, G., Capuano, P., Zollo, A., Scandone, P., 2000. Inferences on the upper crustal structure of the southern Apennines (Italy) from seismic refraction investigations and subsurface data. *Tectonophysics* 317, 273–297.
- Lagabrielle, Y., Bodinier, J., 2008. Submarine reworking of exhumed subcontinental mantle rocks: field evidence from the Lherz peridotites, French Pyrenees. *Terra Nova* 20, 11–21.
- Langston, C.A., 1979. Structure under Mount Rainier, Washington, inferred from teleseismic body waves. *J. Geophys. Res.* 84, 4749–4762.
- Lucente, F.P., Chiarabba, C., Cimino, G.B., Giardini, D., 1999. Tomographic constraints on the geodynamic evolution of the Italian region. *J. Geophys. Res.* 104, 20307–20327.
- Manatschal, G., Muntener, O., 2008. A type sequence across an ancient magma-poor ocean-continent transition: the example of the western Alpine Tethys ophiolites. *Tectonophysics*. doi:10.1016/j.tecto.2008.07.021.
- Martinis, B., Pieri, M., 1964. Alcune notizie sulla formazione evaporitica dell'Italia centrale e meridionale. *Mem. Soc. Geol. Ital.* 4, 649–678.
- Mazzoli, S., Pierantoni, P.P., Borraccini, F., Paltrinieri, W., Deiana, G., 2005. Geometry, segmentation and displacement variations along a major Apennines thrust zone, central Italy. *J. Struct. Geol.* 27, 1940–1953.
- Mazzotti, A., Patacca, E., Scandone, P., Tozzi, M., 1999. Profilo CROP04 Appennino meridionale. Riprocessamento della linea sismica e prim risultati dell'interpretazione. paper presented at FIST Geotitalia, Fed. It Sci. della Terra, Bellaria, Italy, 20 – 23 Sept.
- Menke, W., 1989. Geophysical data analysis: discrete inverse theory. *Int. Geophys. Ser.* 45, 285 Academic, San Diego, Calif.
- Michetti, A.M., Brunamonte, F., Serva, L., Vittori, E., 1996. Trench investigations of the 1915 Fucino earthquake fault scarps (Abruzzo, central Italy): geological evidence of large historical events. *J. Geophys. Res.* 101, 5921–5936.
- Montone, P., Mariucci, M.T., Pondrelli, S., Amato, A., 2004. An improved stress map for Italy and surrounding regions (central Mediterranean). *J. Geophys. Res.* 109, B10410. doi:10.1029/2003JB002703.
- Mostardini, F., Merlini, S., 1986. Appennino centro-meridionale: Sezioni geologiche e proposta di modello strutturale. *Mem. Soc. Geol. Ital.* 35, 117–202.
- Nur, A., 1972. Dilatancy, pore fluids, and premonitory variations of Ts/Tp travel times. *Bull. Seismol. Soc. Am.* 62, 1217–1222.
- Pace, B., Boncio, P., Lavecchia, G., 2002. The 1984 Abruzzo earthquake (Italy): an example of seismicogenic process controlled by interaction between differently oriented synkinematic faults. *Tectonophysics* 350, 237–254.
- Palombo, L., Benedetti, L., Bourlès, D., Cinque, A., Finkel, R., 2004. Slip history of the Magnola fault (Apennines, Central Italy) from 36Cl surface exposure dating: evidence for strong earthquakes over the Holocene. *Earth Planet. Sci. Lett.* 225, 163–176.
- Pantosti, D., D'Addezio, G., Cinti, F., 1996. Paleoseismicity of the Ovindoli-Pezza fault, central Apennines, Italy: a history including a large previously unrecorded earthquake in the Middle Age (860–1300 A.D.). *J. Geophys. Res.* 101, 5937–5959.
- Papanicolaou, I.D., Roberts, G.P., Michetti, A.M., 2005. Fault scarps and deformation rates in Lazio-Abruzzo, central Italy: comparison between geological fault slip rate and GPS data. *Tectonophysics* 408, 147–176.
- Park, J., Yuan, H., Levin, V., 2004. Subduction zona anisotropy beneath Corvallis, Oregon: a serpentinite skid mark of trench parallel terrane migration? *J. Geophys. Res.* 109, B10306. doi:10.1029/2003JB002718.
- Parotto, M., Praturion, A., 1975. Geological summary of the Central Apennines. structural model of Italy. *Quaderni de "La Ricerca Scientifica"* 90, 257–311, C.N.R., Roma.
- Patacca, E., Scandone, P., Di Luzio, E., Cavinato, G.P., Parotto, M., 2008. Structural architecture of the central Apennines: interpretation of the CROP 11 seismic profile from the Adriatic coast to the orographic divide. *Tectonics* 27, TC3006. doi:10.1029/2005TC001917.
- Pialli, G., Barchi, M., Minelli, G., 1998. Results of the CROP 03 deep seismic reflection profile. *Mem. Soc. Geol. Ital.* 52, 1–647.
- Piana Agostineti, N., Chiarabba, C., 2008. Seismic structure beneath Mt Vesuvius from receiver function analysis and local earthquake tomography: evidence for location and geometry of the magma chamber. *Geophys. J. Int.* doi:10.1111/j.1365-246X.2008.03868.x.
- Piccardi, L., Gaudemer, Y., Taponnier, P., Boccaletti, M., 1999. Active oblique extension in the Central Apennines (Italy): evidence from the Fucino region. *Geophys. J. Int.* 139, 499–530.
- Piomallo, C., Morelli, A., 2003. P-wave tomography of the mantle under the Alpine – Mediterranean area. *J. Geophys. Res.* 108. doi:10.1029/2002JB001757.

- Reinen, L.A., 2000. Seismic and aseismic slip indicators in serpentine gouge. *Geology* 28, 135–138.
- Reinen, L.A., Weeks, J.D., Tullis, T.E., 1991. The frictional behavior of serpentinite: implications for aseismic creep on shallow crustal faults. *Geophys. Res. Lett.* 18, 1921–1924.
- Roberts, G.P., Michetti, A., 2004. Spatial and temporal variations in growth rates along active normal fault systems; an example from the Lazzio–Abruzzo Apennines, central Italy. *J. Struct. Geol.* 26, 339–376.
- Roure, F., Casero, P., Vially, R., 1991. Growth processes and melange formation in the southern Apennines accretionary wedge. *Earth Planet. Sci. Lett.* 102 (3–4), 395–412.
- Sambridge, M., 1999a. Geophysical inversion with a neighbourhood algorithm—I. Searching a parameter space. *Geophys. J. Int.* 138, 479–494.
- Sambridge, M., 1999b. Geophysical inversion with a neighbourhood algorithm—II. Appraising the ensemble. *Geophys. J. Int.* 138, 727–746.
- Savage, M., Park, J., Todd, H., 2007. Velocity and anisotropy structure at the Hikurangi subduction margin, New Zealand from receiver functions. *Geophys. J. Int.* 168, 1034–1050.
- Scholz, C.H., 1990. *The Mechanics of Earthquake and Faulting*. Cambridge University Press, New York.
- Scrocca, D., Carminati, E., Doglioni, C., 2005. Deep structure of the southern Apennines, Italy: thin-skinned or thick-skinned? *Tectonics* 24, TC3005. doi:10.1029/2004TC001634.
- Selvaggi, G., Castello, B., Azzara, A., 1997. Spatial distribution of scalar seismic moment release in Italy (1983–1996): seismotectonic implications for the Apennines. *Ann. Geofis.* 40 (6), 1565–1578.
- Sherrington, H.F., Zandt, G., Frederiksen, A., 2004. Crustal fabric in the Tibetan Plateau based on waveform inversions for seismic anisotropy parameters. *J. Geophys. Res.* 109, B02312. doi:10.1029/2002JB002345.
- Speranza, F., Chiappini, M., 2002. Thick-skinned tectonics in the external Apennines, Italy: new evidence from magnetic anomaly analysis. *J. Geophys. Res.* 107 (B11), 2290. doi:10.1029/2000JB000027.
- Thurber, C.H., 1983. Earthquake location and three dimensional crustal structure in the Coyote lake area, central California. *J. Geophys. Res.* 88, 8226–8236.
- Tiberti, M.M., Orlando, L., Di Bucci, D., Bernabini, M., Parotto, M., 2005. Regional gravity anomaly map and crustal model of the Central-Southern Apennines (Italy). *Journal of Geodynamics* 40, 73–91.
- Toomey, D., Foulger, G.R., 1989. Tomographic inversion of local earthquakes data from the Hengill–Grensdalur Central Volcano Complex, Iceland. *J. Geophys. Res.* 94, 17497–17510.
- Tozer, R.S.J., Butler, R.W.H., Corrado, S., 2002. Comparing thin- and thick-skinned tectonic models of the central Apennines, Italy. In: Bertotti, G., Schulmann, K., Cloetingh, S.A.P.L. (Eds.), *Continental Collision and the tectono-sedimentary evolution of forelands*: European Geophysical Union Stephan Mueller Special Publication Series, 1, pp. 181–194.
- Trippetta, F., Vinciguerra, S., Colletini, C., Meredith, P.G., 2008. Physical properties of the seismogenic Triassic evaporites in the northern Apennines (central Italy). *Geophysical Research Abstracts*, v. 10, abs. EGU2-008–A-09990.
- Um, J., Thurber, C.H., 1987. A fast algorithm for two-dimensional seismic ray tracing. *Bull. Seismol. Soc. Am.* 77, 972–986.
- Vezzani, L., Ghisetti, F., 1998. *Carta geologica dell’Abruzzo, 1:100000, SELCA, Via R. Giuliani, Firenze*.
- Vinnik, L.P., Aleshin, I.M., Kiselev, S.G., Kosarev, G.L., Makeyeva, L.I., 2007. Depth localized azimuthal anisotropy from SKS and P receiver functions; the Tien Shan. *Geophys. J. Int.* 169 (3), 1289–1299.
- Wang, Z., Nur, A.M., 1989. *Seismic and Acoustic Velocities in Reservoir Rocks: Volume 2. Theoretical and Model Studies*: SEG Geophysics Reprint Series, No. 10, 457 p.
- Ward, S.N., Valensise, G.R., 1989. Fault parameters and slip distribution of the 1915 Avezano, Italy, earthquake derived from geodetic observations. *Bull. Seismol. Soc. Am.* 79, 690–710.
- Working Group CPTI, 1999. *Catalogo parametrico dei terremoti italiani, ING, GNDT, SGA SSN, Bologna*.
- Zhao, D., Kanamori, H., 1992. The 1992 Landers earthquake sequence: earthquake occurrence and structural heterogeneities. *Geophys. Res. Lett.* 20, 1083–1086.
- Zhao, D., Negishi, H., 1998. The 1995 Kobe earthquake: seismic image of the source zone and its implications for the rupture nucleation. *J. Geophys. Res.* 103, 9967–9986.